Electric Circuit Theory as a method for monitoring tree water deficit at different scales

Georgios Xenakis

Forest Research, Northern Research Station, Roslin, Midlothian, EH25 9SY, UK

Corresponding author. E-mail: georgios.xenakis@forestresearch.gov.uk Telephone: 0044 300 067 5999 Twitter: @drGeorgeXenakis

Electric Circuit Theory as a method for monitoring tree water deficit at different scales

GEORGIOS XENAKIS[1*]

[1]Forest Research, Northern Research Station, Roslin, Midlothian, EH25 9SY, UK

[*]Corresponding author. E-mail: georgios.xenakis@forestresearch.gov.uk Telephone: 0044 300 067 5999

Abstract

Climate change is expected to alter precipitation patterns, making droughts more frequent in some areas, which will expose trees to more severe water deficits which could result in the catastrophic collapse of their water transport system and, eventually, mortality. To inform forest management and tree species suitability to increase forest resilience requires a robust method for understanding the time, duration and impact of water deficits. In this study, I discuss how an application of Electric Circuit Theory (ECT) is a reliable and robust way to detect water deficit in the Soil-Plant-Atmosphere Continuum (SPAC). Based on an electric closed-circuit analogy of the SPAC, I define its "hydraulic efficiency", and when there is a water deficit. Using tree sap flow and evapotranspiration from eddy covariance, I demonstrate the application of the theory and the use of hydraulic efficiency to quantify how long trees and forest ecosystems spend under water deficit conditions. Calculations of ECT-based hydraulic efficiency showed that individual trees of an upland Sitka spruce plantation in N. England spent up to 80% of a monitoring period during the growing season at water deficit in a non-drought year, depending on their location within the stand. The results also showed that before a drought in 2018, the spruce plantation was between 3 and 6% of the time under water deficit, increasing to 31% in the year of the drought and dropping to 16% two years post-drought. Furthermore, using a global database of sap flow measurements, I provide an approach which suggests a way to compare hydraulic efficiency of species in different biomes. This dataset showed 6 out of 10 tropical rainforest species were under water deficit, compared to 5 out of 36 temperate forest species. I discuss how ECT is similar to other supply/loss theories describing tree water relations and conclude that combined with modern technology, it can provide a continuous system for monitoring water deficit.

Keywords: Soil-Plant-Atmosphere Continuum, Electric Circuit Theory, Hydraulic efficiency, Water deficit, Sap flow, Ecosystem evapotranspiration.

1   Introduction

The climate is changing, and intra-annual and inter-annual precipitation patterns are changing (Zhou et al., 2019). Trees can respond to environmental changes because of their physiological plasticity (Kramp et al., 2022), although evolutionary responses to changes in the climate can take hundreds of years, and the rapid changes in precipitation are giving limited time for trees to adapt. These changes can result in severe water deficits impacting tree species performance, leading to the catastrophic collapse of the tree water transport system (Arend et al., 2021) and, ultimately, canopy dieback (Losso et al., 2022) or tree mortality (McDowell et al., 2008; Rowland et al., 2015; Choat et al., 2018). In order to enhance forest resilience and thereby preserve future forest resources, a quick and reliable method for quantifying water deficit is required to inform forest management decisions on species suitability and drought hazard risk (van Oijen and Brewer, 2022).

Traditionally tree ecophysiological assessments of water stress use leaf-level gas exchange (e.g., Rehschuh et al., 2020), leaf turgor loss (e.g., Zhu et al., 2018) or plant trait assessments such as hydraulic safety and efficiency (e.g., Schumann et al., 2019; Fuchs et al., 2021a). These approaches offer reliable measurements at the plant level, giving valuable insights into water regulation mechanisms and quantification of individual species response (Irvine et al., 1998). However, because of their mostly laboratory or leaf-based application, they offer data for a limited range of environmental and growing conditions that are not sufficient to explore interactions of the whole soil-plant-atmosphere-continuum (SPAC) during water-limited periods.

There are also other approaches and indices developed for monitoring drought and water deficit. Many studies use transpiration (Nadezhdina, 1999), leaf water potential (Nel and Berliner, 1990), relative soil water content (Granier et al., 2000), canopy temperature (Reinert et al., 2012; Drechsler et al., 2019), stem shrinkage (Zweifel et al., 2005; Alizadeh et al., 2021), tree sway (Ciruzzi and Loheide, 2019) or energy balance models (Nieto et al., 2022). Remote sensing is commonly used to detect drought at the stand or regional scales with spectral (Yang et al., 2020) or radar sensors (Konings et al., 2021). However, to the best of my knowledge, there is no method

that offers a way to capture all the fundamental drivers that lead to water deficit and potential stress in a continuous, simple, cost-effective, robust and real-time method applicable at different scales.

It is well known that vapour pressure deficit is the main driver for water loss, movement and uptake (Grossiord et al., 2020) and hence one of the factors directly affecting water deficit levels, whilst soil water potential regulates stomatal closure (Carminati and Javaux, 2020). In order to develop a more broadly applicable and site-specific way of accessing water deficit and subsequently stress, I propose a method that integrates across the SPAC holistically by representing three key elements: 1) quantify the resistance of the plant and assess how it changes over time as water deficits increase, 2) quantify the soil water available for plant uptake and 3) quantify the force the atmosphere applies across the SPAC and how it affects the levels of water deficit plants are experiencing.

Electrical engineering theory offers suitable analogies to fulfil all three elements successfully. Although many mechanistic models already have adopted electric circuits to represent water movement through the soil-plant continuum (Landsberg et al., 1976; Milne et al., 1983; Hunt et al., 1991; Williams et al., 2001; Zhuang et al., 2014), their detailed approach does not offer an in-situ quantification of the timing, duration and intensity of water deficit and potential stress. So, we must look further into using some electrical engineering principles, also known as Electric Circuit Theory (ECT) to devise a metric. Analogies of ECT have been used in other aspects of science, such as connectivity and conservation (McRae et al., 2008; Dickson et al., 2018), plant and animal genetics (McRae and Beier, 2007) and biochemistry (Tang et al., 2021). Here, I am extending some further ECT analogies into tree ecophysiology and, particularly, water movement that has yet to be explored.

1.1   The proposed concept

I propose to adopt and adapt Electric Circuit Theory to determine the "hydraulic efficiency" of the SPAC. This novel application enables the definition of a single index to identify the point at which transpiration losses balance with soil water supply. Knowing when water transport is balanced allows for a quantified estimate of how long plants have been exposed to water deficit. Hydraulic efficiency must not be confused with water use efficiency since the former considers water trans-

port through the SPAC.

By adapting two concepts from ECT, electric power and efficiency, I propose to define the hydraulic power of the SPAC as the energy required for moving water across a water potential gradien per unit of time. Furthermore, I propose that hydraulic efficiency is defined as the power used by the plant divided by the total power of the SPAC or simply the ratio of energy required for water movement in the plant to the total energy of water flow in the SPAC.
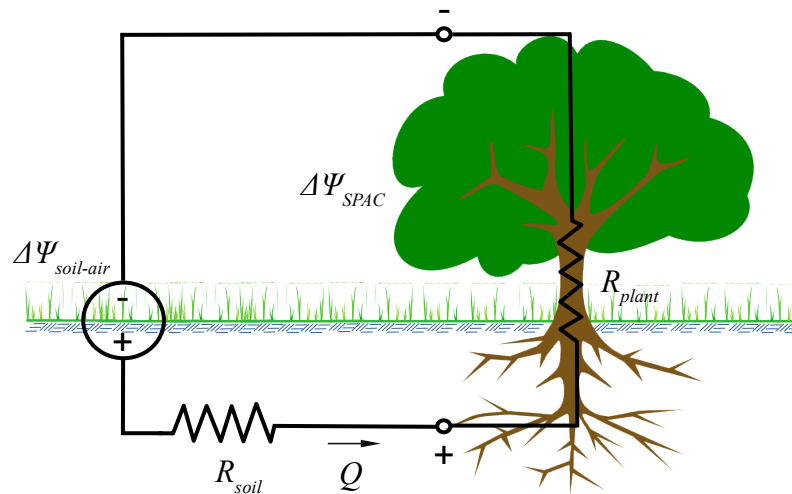
Figure 1: An electric closed-circuit analogy of the soil-plant-atmosphere continuum (SPAC) for water flow with two resistors (R_{soil} and R_{plant}) and one source ($\Delta\Psi_{soil-air}$). $\Delta\Psi_{SPAC}$ is the water potential difference of the SPAC (see Equation 2).

1.1.1 The electric closed-circuit analogy

Within the SPAC, I represent the water movement at a tree scale with a simple closed electric circuit of two resistors and one source (Figure 1). This simplification allows the estimation of water deficit based on continuous and reliable measurements of three circuit elements.

Since atmospheric vapour pressure deficit controls stomatal conductance and hence the movement of water, I consider atmospheric water potential rather than leaf water potential as the "negative" term of the potential difference (Figure 1). Similarly, I consider soil water potential as the "positive" term of the potential difference, thereby representing a flow or a "battery". Note, the potential difference is between soil and atmosphere without the plant. Precipitation is a recharging event of the source "battery". The two resistors of this simplified electric circuit analogy are

the soil and plant. I assume that tree stem resistance is sufficient to represent plant resistance (Jones, 1992; Zhuang et al., 2014), as the longest water conducting pathway. The advantage of this approach is that all elements can be derived from continuous measurements of soil water, transpiration, air temperature and relative humidity. Although the closed-circuit analogy of Figure 1 is based on tree-level hydraulics, a similar analogy can be made at an ecosystem level, where transpiration is replaced by evapotranspiration.

1.1.2 Calculation of hydraulic efficiency

Using Ohm's law, we calculate the flow of water (Q) as the ratio of the difference in water potential between soil and the atmosphere to the sum of soil and plant resistance (Equation 1).

$$Q = \frac{\Delta \Psi_{soil-air}}{R_{soil} + R_{plant}} \tag{1}$$

According to the voltage divider rule, which states that the voltage across any resistor connected in series is equal to the product of the total supply voltage and the resistance of the resistor divided by the total resistance of the circuit, we can calculate the difference in water potential of the soil-plant-atmosphere continuum (SPAC) using Equation 2.

$$\Delta \Psi_{SPAC} = \Delta \Psi_{soil-air} \frac{R_{plant}}{R_{soil} + R_{plant}} \tag{2}$$

Since the power produced by a load resistor in an electric circuit is the product of voltage and current, similarly, we calculate the power of the SPAC as the product of $\Delta \Psi_{SPAC}$ and the water flow Q (Equation 3).

$$P_{SPAC} = \Delta \Psi_{SPAC} Q = \frac{R_{plant} \Delta \Psi_{soil-air}^2}{(R_{soil} + R_{plant})^2} \tag{3}$$

Substituting $\Delta \Psi_{SPAC}$ in Equation 3 with Equation 2, we determine the SPAC power using its resistance and the water potential difference between soil and air ($\Delta \Psi_{soil-air}$). Replacing R_{plant} with R_{stem} and rearranging to remove R_{stem} from the numerator, the hydraulic power of the plant

is given by Equation 4.

$$P_{plant} = \frac{\Delta\Psi^2_{soil-air}}{R_{soil}\left(\frac{\sqrt{R_{soil}}}{\sqrt{R_{stem}}} + \frac{\sqrt{R_{stem}}}{\sqrt{R_{soil}}}\right)^2} \tag{4}$$

Similarly, we calculate soil power with Equation 5.

$$P_{soil} = \frac{\Delta\Psi^2_{soil-air}}{R_{stem}\left(\frac{\sqrt{R_{soil}}}{\sqrt{R_{stem}}} + \frac{\sqrt{R_{stem}}}{\sqrt{R_{soil}}}\right)^2} \tag{5}$$

Finally, we calculate the hydraulic efficiency as the ratio of the plant's power to the sum of soil and plant power (Equation 6).

$$\eta = \frac{P_{plant}}{P_{plant} + P_{soil}} \tag{6}$$

1.1.3 Thresholds of hydraulic efficiency classes

Before assessing when and for how long trees were exposed to water deficit, it was crucial to set some theoretical hydraulic efficiency thresholds. By its definition, the new ECT-based hydraulic efficiency is a dimensionless quantity which quantifies the balance between the transpirational demand and soil water supply (Sperry and Love, 2015). The advantage is its inherent optimisation point, known as the Maximum Power Transfer (MPT, Figure 2), where plant xylem and soil resistance are equal and $R_{plant}/R_{soil} = 1$. The second advantage is that MPT can be identified from timeseries data using widely available measurements from sap flow and soil water potential/content sensors.

The response function suggests that when $R_{plant}/R_{soil} > 1$, the water supply is greater than transpiration. Similarly, when $R_{plant}/R_{soil} < 1$, water loss exceeds supply. We can then assign η thresholds for defining efficiency classes. At the point of MPT, the response function shows that η = 0.5. Starting from there and allowing a 30% variation on both sides, I defined the "most efficient" water transport (η_{me}) to span efficiency ratings $0.412 < \eta \leq 0.565$. The 30% on either side of MPT is a reasonable assumption that allows the slope of the hydraulic efficiency function within the most efficient class to reflect water balance, as presented in the stomatal optimisation model by Sperry et al. (2017). Their model assumes that stomata maintain optimum transpiration when canopy pressure is such that both carbon gain and soil water supply are in balance (Sperry
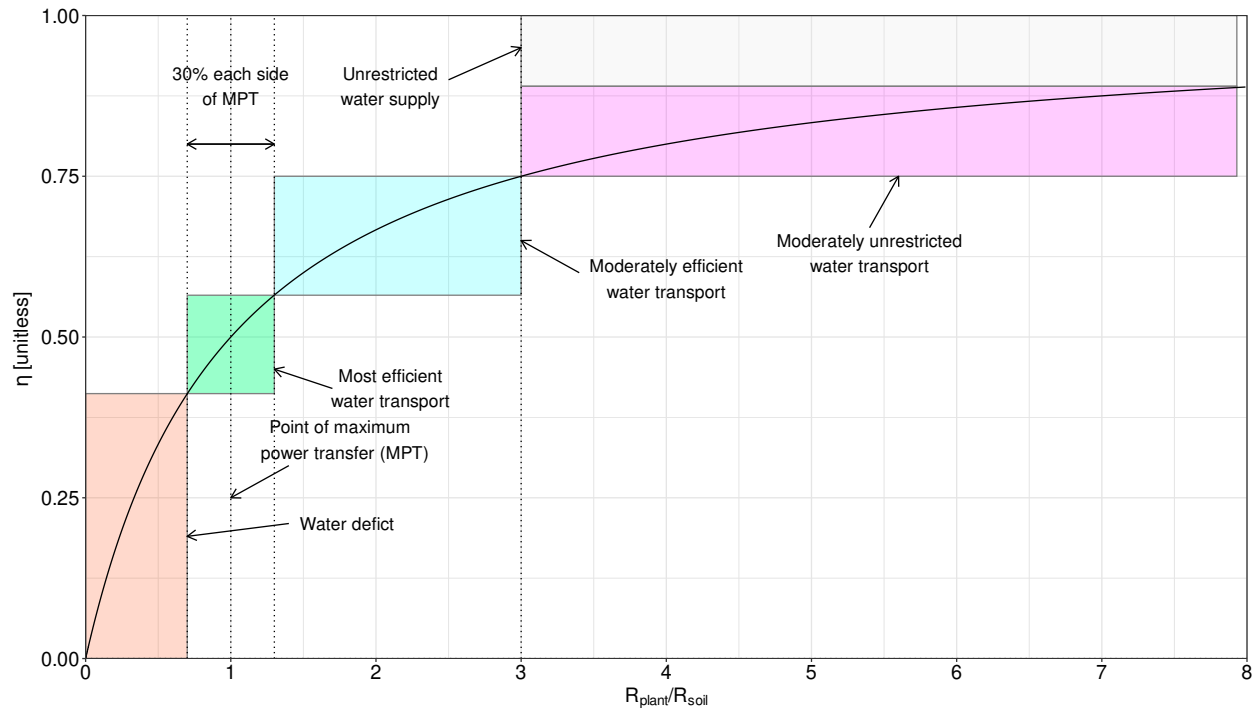
Figure 2: Response function showing the relationship between the ratio of the plant (R_{plant}) to soil (R_{soil}) resistance and hydraulic efficiency. The Maximum Power Transfer (MPT) is defined as the point where the ratio equals one (Rplant = Rsoil). Assuming a 30% variance around the MPT we classify hydraulic efficiency in five classes including water deficit ($0 < \eta_{wd} \leq 0.412$), most efficient ($0.412 < \eta_{me} \leq 0.565$), moderately efficient ($0.565 < \eta_{mde} \leq 0.75$), moderately unrestricted ($0.75 < \eta_{mu} \leq 0.89$), and unrestricted water transport ($0.89 < \eta_{u} \leq 1$). Each class is colour-coded, and the same scheme is used throughout the illustrations.

et al., 2017, Figure 1b). Assuming this is the maximum power transfer point for water movement, deviating 30% has similar implications for water transport, with a decrease suggesting stomatal limitation resulting in lower transpiration in response to lower water supply. The class for "water deficit" (η_{wd}) is defined as $\eta \leq 0.412$. Conversely, when plant water resistance is three times the soil water resistance, a point when the slope of the response function becomes small, we can consider water supply as unrestricted. When $0.565 < \eta \leq 0.75$ the hydraulic efficiency is defined as "moderately efficient" (η_{mde}), with anything between $0.75 < \eta \leq 0.89$ as "moderately unrestricted" (η_{mu}). For $\eta > 0.89$, I considered it as "unrestricted" water supply (η_u).

1.2   Objectives and aim of the study

In this study, based on the new proposed definition of hydraulic efficiency, I will first provide a theoretical framework for determining when trees are most efficient at water uptake. Then, using

field measurements at the tree level, I will apply the theoretical framework to investigate how long a tree spends under water deficit conditions. Furthermore, using eddy covariance data, I will apply the same principles at the ecosystem level and focus on a recent drought that occurred in a mature stand of trees. Finally, using a global database of sap flow measurements, I will assess the hydraulic efficiency of several species across various forest biomes and discuss what it means for their water regime under a future water-limited climate.

The overall aim is to demonstrate the practical application of Electric Circuit Theory and develop a methodology for quantifying the efficiency of water transport through the SPAC at different spatial scales (tree, stand & biome). Furthermore, this study aims to provide a means of quantifying the period of water deficit.

2   Material and methods

The theoretical focus of this study requires a range of data, from tree to ecosystem and biome level. Therefore, I used data from tree-level field measurements, long-term ecosystem and meteorological data from an intensively monitored flux site and a sap flow measurements database. All data manipulation, calculations, analyses and graphics were performed using the R software (R Core Team, 2022) and its associate packages.

2.1   Study site

The Harwood Forest Conifer Research Platform is a flux monitoring site at a commercial upland conifer plantation in Northumberland, North-East England. The data used here are from a 40 ha second rotation, even-aged, mature Sitka spruce (*Picea sitchensis* (Bong.) Carr.), planted in 1973 on peaty-gley (cambic stagnohumic gley, WRB, FAO) soils. The top height of the stand was 26 m, with a mean tree density of 1348 trees ha^{-1} and a leaf area index of 5.7. The site's elevation is 290 m with a slope of 2°. In 2014, a 32 m scaffolding tower was installed to monitor the carbon, energy and water fluxes with eddy covariance. For more information about the site, see Xenakis et al. (2021).

2.2 Data sources

2.2.1 Sap flow

In May 2021, ten sap flow sensors (Figure 3, SFM1, ICT International Ltd., Australia) were installed assessing individual tree water flow using the heat pulse method (Burgess et al., 2001). Trees were selected using a stratified sampling from a survey of tree diameter from two transects within the footprint of the tower, with thirteen 5 m radius plots. Data were then split into five diameter classes between 7 and 57 cm. Two sensors per diameter class were installed on trees with the median diameter for the class. Before installation, a 5 mm diameter tree core was extracted with a Pressler borer, and the sapwood was stained with indicator dye to calculate the sapwood area. Sensors were installed following manufacturer instructions (Burgess and Downey, 2014) at breast height (1.3 m).

Figure 3: SFM1 sensor used to measure stem sap flow in-situ in a Sitka spruce tree in a mature upland plantation at the Harwood Forest site, N. England.

Heat velocity was calculated every 10 minutes in each tree between May and August 2021, recorded on the onboard logger of each sensor device. Velocity was measured in two points across the 35 mm long needle to capture any variability within the sapwood. Calculated sap velocity was corrected for tree wounding during installation. Before data processing, sap velocities were corrected for offset due to needle misalignment. To calculate the offset for each tree and each of the two measurement points along the needle, mean sap velocity across the measurement period for nights when the vapour pressure deficit was close to zero was obtained. Sap flow was then calculated for each tree from the sapwood area split into two annuli based on the measurement depth of each point along the 35 mm needle (cf. Burgess and Downey, 2014). If the sapwood area was larger, and there was a leftover area unaccounted for, a linear interpolation

was applied to estimate the sap flow form the inner point of the sensor to the end of the sapwood. Due to technical issues, only six of the ten trees gave good quality data during the measurement period.

2.2.2   Eddy covariance and meteorology

Evapotranspiration fluxes were measured with a conventional eddy covariance system at a frequency of 10 Hz set up at 33 m above ground between 2015 and 2018 and at 38 m between 2019 and 2020 and associated air temperature, relative humidity, and precipitation measured every 5 s and aggregated into 30-minutes to match the flux data. For a detailed description of the equipment, set-up, data processing, and corrections, see Xenakis et al. (2021).

2.2.3   Soil water content

The soil water content near each of the ten trees was monitored with CS650 time-domain reflectometry sensors (Campbell Scientific Ltd., Shepshed, Leicestershire, UK). The sensors were placed vertically into the soil surface, approximately 20 cm away from the stem of each tree, and data were recorded with a CR1000 data logger (Campbell Scientific Ltd.). The length of the sensor is 30 cm, so we can assume values are the mean soil moisture of this depth. For ecosystem level calculations, the mean soil moisture from six CS605 sensors (Campbell Scientific Ltd.) placed in a vertical direction every 5 m along a transect starting from the foot of the tower (Xenakis et al., 2021) were used.

2.2.4   SAPFLUXNET

Data from the SAPFLUXNET database version 0.1.5 (Poyatos et al., 2021) was used to represent the broader biome assessment The SAPFLUXNET database contains 202 timeseries for 174 tree species. In addition, the database is accompanied by the "sapfluxnetr" R package, which allows accessing and extracting data and metadata at different temporal scales.

For this study, five biomes are represented: temperate forests, temperate grassland deserts, tropical forest savannas, tropical rainforests, and woodland/shrublands. Extracted daily sapwood area-based time series of sap flow, soil moisture, air temperature and humidity, and soil texture information for each forest type were collated. Sites with no soil moisture data or soil texture

information were excluded from the analysis. The final dataset contained time series from 71 sites across 20 countries.

2.3   Additional calculations and analysis

Soil water potential was calculated using the generalised equations of Saxton et al. (1986) from volumetric water content. Sand and clay proportions for Harwood Forest were set to 40% and 15%, respectively, following calibration of the process-based model 3PG-SoNWaL for the same volumetric soil water content data (Morris et al. 2023, in preparation). To calculate $\Delta\Psi_{soil-air}$, volumetric water content for soil without trees was calculated based on data of a forested and a felled stand (Xenakis et al., 2021) of the same soil type and microclimate. Atmospheric water potential was calculated from air temperature and humidity using the ideal gas law.

Soil resistance was calculating as the inverse of soil conductance. Soil conductance was calculated from soil conductivity (Saxton et al., 1986) and measured volumetric water content, assuming water flows in a "pipe" of soil of 1 m length and 1 m^2 surface area. Plant resistance was also calculated as the inverse of plant conductance. It was assumed stem resistance is sufficient to represent whole-plant resistance. Plant conductance was calculated from sap flow and $\Delta\Psi_{SPAC}$.

Similar calculations were applied for the SAPFLUXNET. If sand and clay percentage was missing from each site's metadata, a default value was set using each site's soil texture description. The default value was the mid-point for each soil texture description in the USDA soil texture classification triangle (USDA, 1987). The site was excluded from the analysis if the soil texture description was missing.

After calculating η for all datasets, empirical cumulative distribution functions (ECDF) using the ecdf function of the ggplot2 package were obtained and plotted against the calculated efficiency. From the intersection between the ECDF and the four η thresholds (see section 1.1.3), the total percentage (of tree and ecosystem level measurements) within each hydraulic efficiency class was obtained. Multiplying the percentage with the total number of days of the sample collection gave the duration in each category. Finally, for the SAPFLUXNET sites, the mean η per species was calculated and plotted against the five categories to assess each species' overall hydraulic efficiency.

3   Results and discussion

3.1   Hydraulic efficiency classes

The hydraulic efficiency classes prescribed are not equidistant but dependent on the slope of the response function (Figure 2). The response function shows a sharp decline in efficiency when $\eta \leq 0.412$, suggesting that when efficiency drops below 30% of MPT, transpiration driven by high vapour pressure deficit increases to such an extent that soil water is depleted rapidly. Eventually, as the soil dries, transpiration ceases, resulting in no water movement; hence $\eta = 0$. Theoretical work on demand/supply (Sperry and Love, 2015; Sperry et al., 2017) strongly support my proposed hydraulic efficiency theory under water deficit conditions. Sperry and Love (2015)), using a supply/loss theory, showed a sharp decline in transpiration as the soil dried. Sperry et al. (2017) developed the theory further. They identified the optimum stomatal point when water supply and carbon gain are in balance, which confirms the maximum power transfer as the point of optimal stomatal regulation and efficient water movement. Although the hydraulic efficiency I present here does not inherently include photosynthetic capacity, Sperry et al. (2017) findings infer that optimal carbon gain must be achieved during MPT. It also explains what the water deficit class of hydraulic efficiency represents. As canopy pressure increases, xylem water movement increases, with stomatal conductance being the limiting factor, despite the high carbon gain, until a critical point is reached when vulnerability to cavitation increases. Continuing transpiring at high rates will lead to a drop in soil water availability and hydraulic efficiency. Based on this theory, maximum stomatal conductance is achieved within the water deficit class. The close theoretical basis between the ECT-based hydraulic efficiency and the supply/loss theory of Sperry and Love (2015) and Sperry et al. (2017) provides additional theoretical validation for its application as a water deficit index. The advantage of ECT is its simplicity, which allows continuous, non-destructive and real-time monitoring of water deficit and identification of periods of optimum water conditions for growth.

Despite the strong theoretical basis of this new index, further work is needed to establish it as the methodology for answering some fundamental questions regarding the impacts of water deficits and drought events. For example, it is known that prolonged exposure to water-limited conditions increases the probability of embolism (Arend et al., 2021), which can lead to mortal-

ity (Rowland et al., 2015; Choat et al., 2018). However, more information is needed about the minimum length of water deficit or how many water-limited periods trees are exposed to before critical limitations to growth or mortality occur, which is likely to be functional type or species specific. Water manipulation experiments combining measurements of hydraulic efficiency and plant physiological traits (e.g., photosynthetic capacity or water use efficiency) will help confirm when water deficit impacts on tree physiology occur, how severe or how prolonged, and ultimately help us understand if water limitation or carbon starvation is the primary driver of mortality.

3.2   Tree level

The simplistic theoretical basis of ECT hydraulic efficiency makes it applicable at different scales. At the tree scale, it is helpful to highlight water deficit periodicity. Figure 4 shows the sap flow, soil water and hydraulic efficiency for three of the six sample trees monitored at Harwood Forest
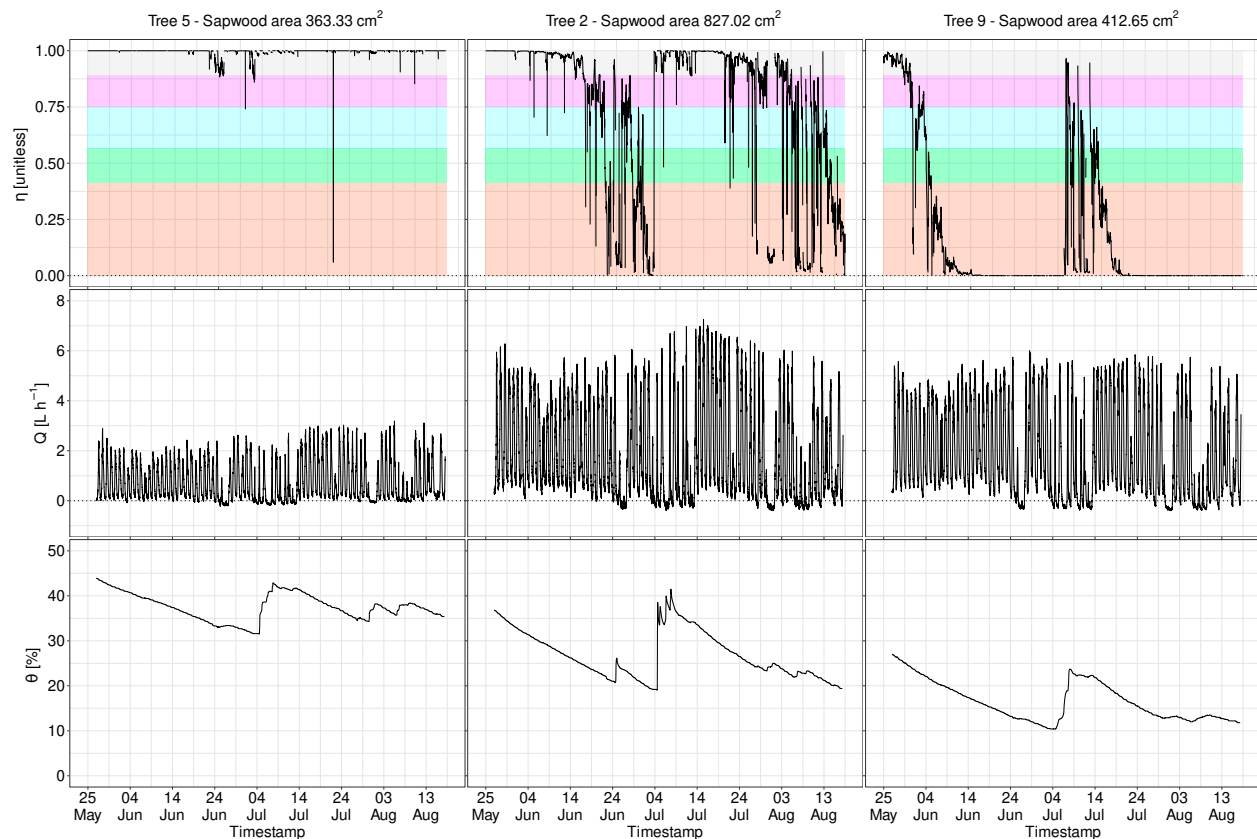
Figure 4: Hydraulic efficiency (top, η unitless), sap flow (middle, Q, $\mathrm{L\,hr^{-1}}$) and volumetric water content (bottom, θ, %) for three trees in Harwood Forest, Northumberland N. England, with different levels of soil water. Colour bands in the top three panels correspond to the colour-coded hydraulic efficiency classes shown in Figure 2.

between the end of May and mid-August in 2021. Three trees are highlighted in the analysis as exemplars of efficiency shifts due to the magnitude of transpiration and soil moisture change measured in-situ.
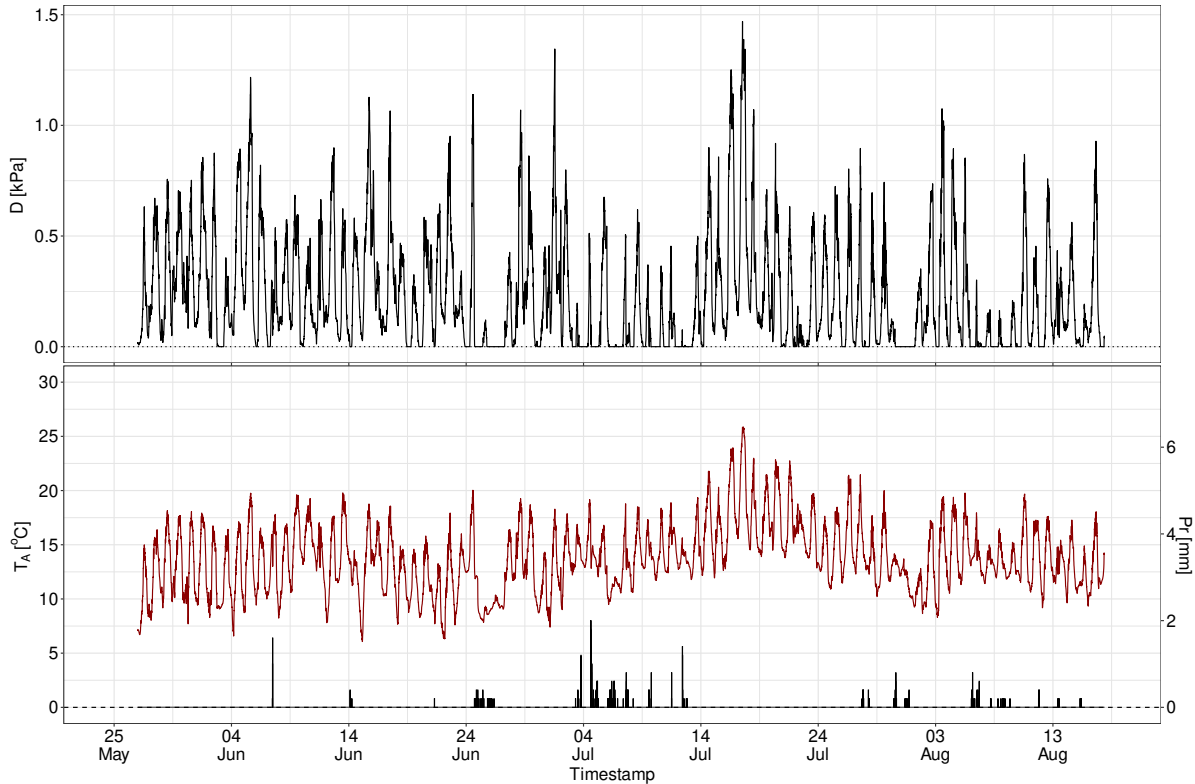
Figure 5: Timeseries of 10-min vapour pressure deficit (D, kPa), air temperature (T_A, $^o\mathrm{C}$) and total precipitation (Pr, mm) during the period of sap flow measurements between May and August 2021 at Harwood Forest, Northumberland. All variables were measured over the forest canopy at $32\,\mathrm{m}$ above the ground.

Tree number 2 had the greatest sapwood area of the three, with 826 cm^2, followed by trees 9 and 5, with 413 and 363 cm^2, respectively. Before a long rainy period in early July, transpiration reduced soil water content for all three trees but at different levels with approximately 30, 20 and 10% minimum θ for trees 5, 2 and 9, respectively. The difference in soil water content is because of their location within the stand. Tree 5 was in a flat, less well-drained part of the stand, tree 2 was on a slope of about 1°, and tree 9 was close to a gap in the canopy. For tree 5, the combination of low transpiration and flat terrain resulted in the higher soil water content. For tree 2, the slope likely contributed to diminishing soil water status, due to drainage. However, for tree 9, the gap allowed more light to reach lower in the canopy and the ground, and possibly more air movement, increasing the evaporation and transpiration components and resulting in lower soil availability.

The magnitude of measured sap flow in this study was typical for Sitka spruce. Beauchamp et al. (2013) found sap flow of a Sitka spruce tree with a similar sapwood area to that of tree 9 (419 cm^2) transporting 4.3 $\mathrm{L}\ \mathrm{h}^{-1}$ during August, very close to the value of 4 $\mathrm{L}\ \mathrm{h}^{-1}$ found here. The high sapwood area meant tree 2 transpired up to 7 $\mathrm{L}\ \mathrm{h}^{-1}$ after the rainfall event between the 4 and 14 of July replenished the soil water reservoir (Figure 5). The increase in transpiration after the rainfall was driven by an increase in vapour pressure deficit (Figure 5).

Calculations of the hydraulic efficiency showed that tree 5 did not reach the water deficit thresholds throughout the sampling period. Hence its water transport was efficient although small (2-4 $\mathrm{L}\ \mathrm{h}^{-1}$). Out of the three, tree 9 reached a large water deficit with a prolonged period of η being close to zero (Figure 4). Both trees 2 and 9 reached the threshold water deficit prior to the rainfall event, with drought onset for tree 9 occurring more rapidly (Figure 4 and 6). During the rainfall event, efficiency increased due to high water availability and low transpiration, meaning water movement, although small, was unrestricted. After the rainfall event, efficiency started to drop again, getting closer to the moderate and most efficient hydraulic efficiency classes for both
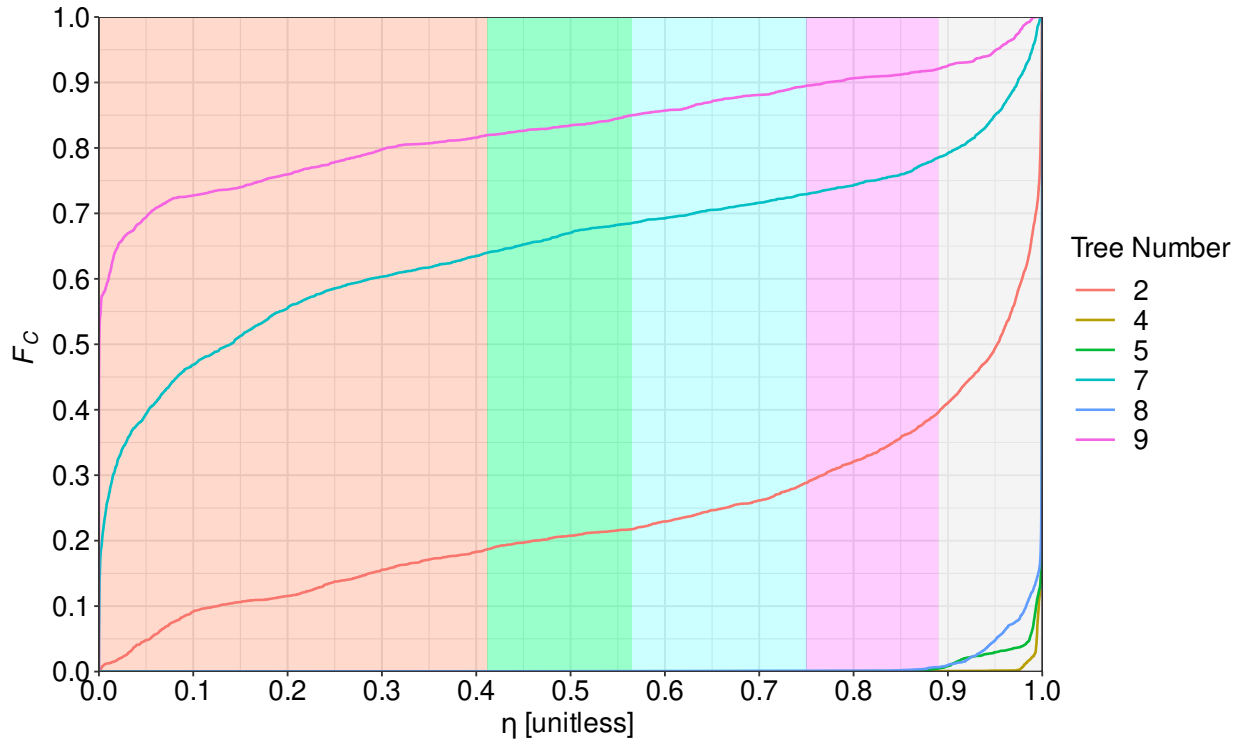
Figure 6: Empirical cumulative density functions (F_C) of hydraulic efficiency (η) plotted against efficiency for the six Sitka spruce trees measured in Harwood Forest that had complete time-series over the monitoring period. Colour bands correspond to the five hydraulic efficiency classes.

Table 1: Number of days (N) tree and ecosystem hydraulic efficiency was classified as water deficit (η_{wd}), most efficient (η_{me}), moderately efficient (η_{mde}), moderately unrestricted (η_{mu}) and unrestricted classes (η_{mu}), and the mean efficiency ($\overline{\eta}$) during the monitoring period of Sitka spruce trees in N. England. The number in parenthesis is the standard error of the mean. The number of days was calculated for individual trees and for each year of available flux data at the ecosystem level.

	N_{η_s}	$N_{\eta_{me}}$	$N_{\eta_{md}}$	$N_{\eta_{mu}}$	N_{η_u}	$\overline{\eta}$
			Tree level			
2	15	2	6	10	49	0.78
4	-	-	-	-	82	1
5	-	-	-	-	81	0.99
7	52	4	4	5	18	0.36
8	-	-	-	1	82	0.99
9	67	3	4	2	7	0.17
			Ecosystem level			
2015	13	5	11	36	301	0.91
2016	21	3	7	18	315	0.91
2017	24	11	15	32	283	0.88
2018	115	32	38	38	143	0.63
2019	43	27	35	66	195	0.79
2020	49	19	31	45	222	0.8

trees 2 and 9. Noticeable, however, is how quickly tree 9 returned to the water deficit class after the rainfall event despite soil water going up to about 22%. Xenakis et al. (2021) found that the average soil moisture for the stand during the extreme drought of 2018 was 23% at a comparable soil depth. Soil water around tree 9 seemed to be below the average of a drought period, which suggests, despite the high rates of transpiration (4-6 $\mathrm{L\ h^{-1}}$), the tree has been exposed to prolonged water deficit conditions and hence more likely to suffer from either catastrophic xylem failure (McDowell et al., 2008; Brodribb and Cochard, 2009; Arend et al., 2021).

To assess the total time spent under water deficit conditions with ECT-based hydraulic efficiency we can employ empirical cumulative density functions (ECDF, Figure 6). This indicates that for 70% of the monitoring period, tree 9 showed an efficiency of less than 0.1, with 82% within the water deficit class (67 out of 82 days of monitoring, Table 1). Tree 2 was only 15 days in the "water deficit" class (18.4% of the sampling period). Both trees spent two to three days in the "most efficient water transport" class (Table 1). On the other hand, tree 2 was 49 days in the "unrestricted water transport" class, while tree 9 was only seven days. Out of the six trees monitored, four were more than 50% of the time within the unrestricted water transport class and had a mean η of more than 75% (Table 1). The organo-mineral peaty gley soil retains moisture preventing trees from

being within the most efficient water transport class. Under future climatic drought, Sitka spruce is expected to become water stressed relatively quickly because of its poor stomatal control (Beadle et al., 1978). Monitoring hydraulic efficiency at individual tree-level assessments both in the field and during in-situ manipulation experiments could provide better understanding of the impact of repeated water deficit on growth and survival.

3.3   Ecosystem level

Hydraulic efficiency, calculated at the ecosystem level using six years of eddy covariance data, showed evident water deficit during 2018 (Figure 7). The stand was under water deficit for 115 days (31% of the year) and 143 (40% of the year) unrestricted (Table 1). During 2018, the stand spent 9% of the year in the most efficient class, the highest out of the six years. The three years before the drought the stand was under water deficit between 3 and 6% of the year, while the two years after drought was between 11 and 16%.
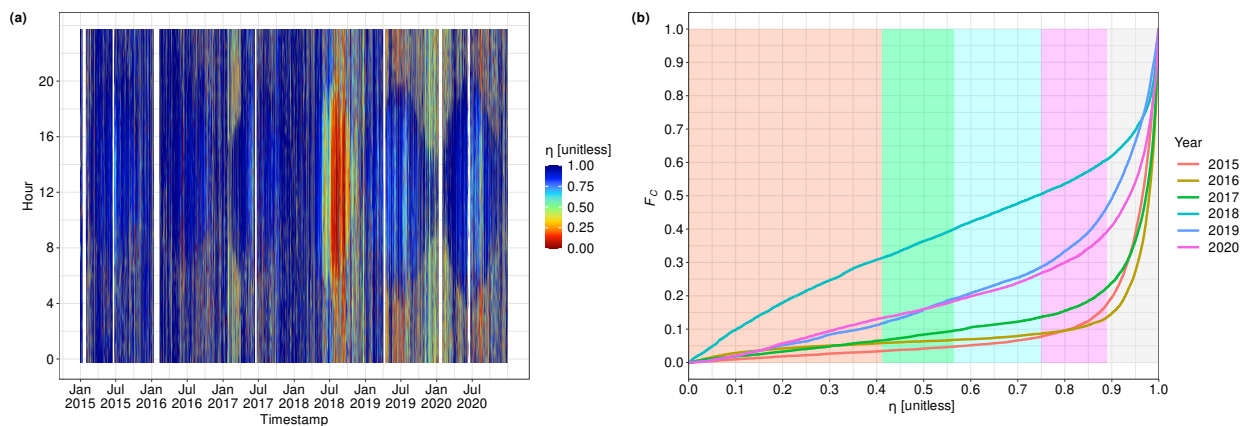
Figure 7: Fingerprint plot (a) and empirical cumulative density functions (b) for stand level hydraulic efficiency calculated from evapotranspiration measurements from the eddy covariance tower at Harwood Forest, Northumberland. The colour bands in panel (b) correspond to the hydraulic efficiency classes.

Water transport became more efficient for 32 days as the site was initially drying (Table 1). However, as the site continued to dry, it entered a prolonged water deficit period that resulted in 7% less photosynthesis and a drop in inherent water use efficiency by 73% compared to the previous three years (Xenakis et al., 2021). In the following two years, the stand spent less time under water deficit conditions which helped the recovery of photosynthesis to 2015 levels over the subsequent two-year period (data not shown) (Aubinet et al., 2018).

Annual ECDF analysis of the hydraulic efficiency with the results by Xenakis et al. (2021) showed that Sitka spruce achieved high levels of photosynthesis $(84 - 92 \ \mathrm{tCO2e\,ha^{-1}})$ under unrestricted water availability. However, when the stand was under water deficit for a third of the year, there was a significant drop in carbon uptake and water use efficiency, despite the small drop in photosynthesis. This has implications for tree growth and forestry contributions to government national net zero targets under future climate (Bateman et al., 2022), where droughts will become more frequent and water resources more sparse (Zhou et al., 2019). Therefore, it is important to continue monitoring water deficit at ecosystem level using existing eddy covariance flux sites and ECT-based hydraulic efficiency index.

3.4   Biome level

Drought-related research focuses on understanding the mechanisms developed by trees to manage available water resources effectively (Martínez-Vilalta et al., 2014; Sperry and Love, 2015; Sperry et al., 2017; Mencuccini et al., 2019). Analysis of global datasets often offers a broader range of variability, helping investigation of fundamental water regulation mechanisms within the soil-plant continuum. At the biome level the ECT approach enables a comparison of species efficiency with respect to hydraulic mechanisms. The implication is that less efficient species may become hydraulically compromised more rapidly under water deficit especially where limited natural adaptation occurs due to rapid climate changes. Hence, the ability to develop indices which identifying species that are resilient to limited water resources are required.

The proposed method enables the quantification of the hydraulic efficiency for a wide range of species across five biome types. Figure 8 illustrates the mean η for each species during their respective measurement period. The analysis shows that measurements for most forest species in the temperate zone indicated that $\eta > 0.75$ (5 out of 36). Values for two species were "most efficient" in water transport $(0.412 < \eta \leq 0.565)$, and five were under "water deficit" $(\eta \leq 0.412)$. The calculated mean η value for most of the tropical forest biome species were within the "water deficit" class (6 out of 10 species).

The mean efficiency of Sitka spruce was in the "unrestricted hydraulic efficiency" class, which confirms ecosystem-level findings (Xenakis et al., 2021), as it is usually growing in wet soil conditions with transpirational losses rarely exceeding available water. The mean hydraulic efficiency
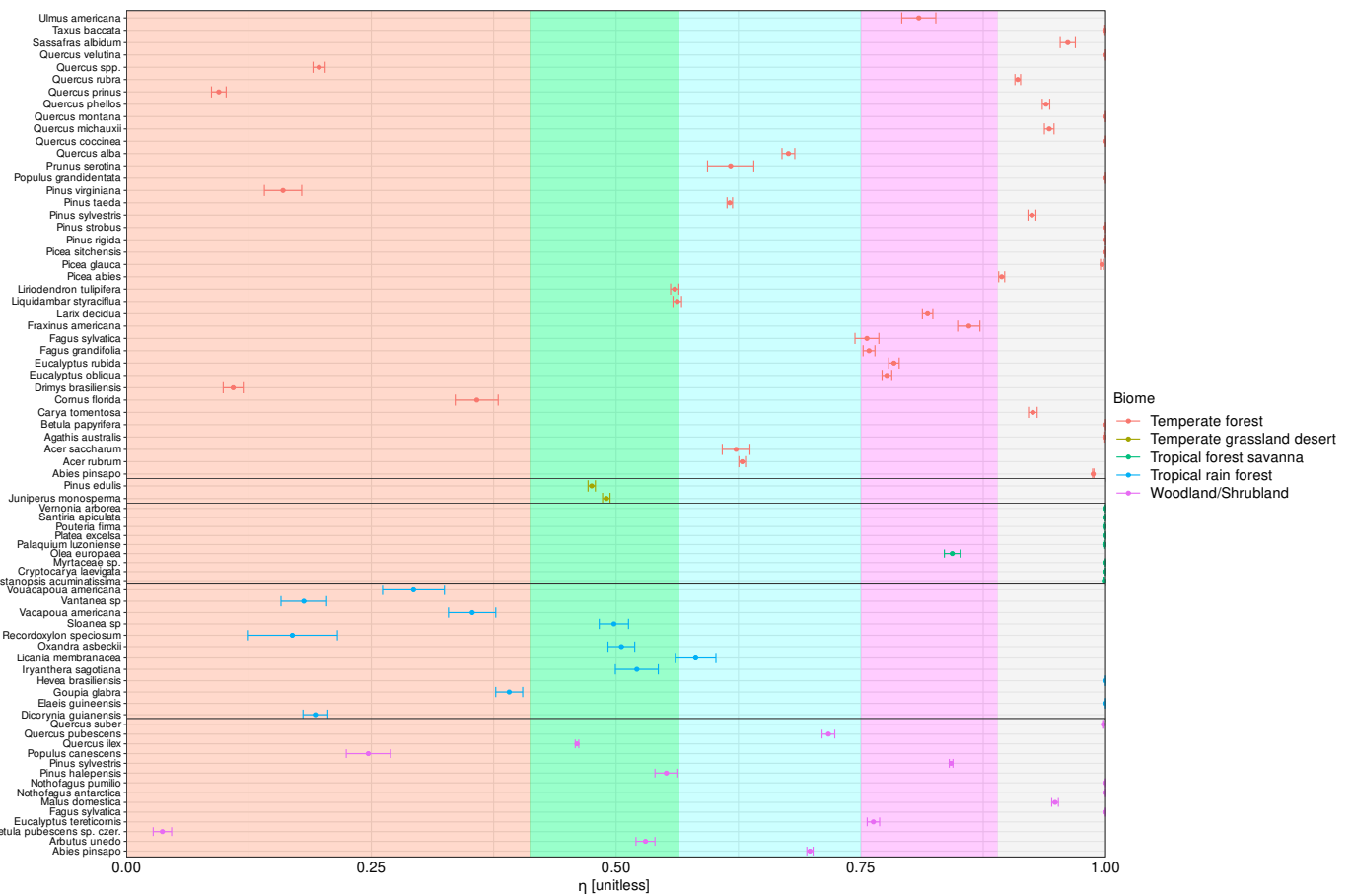
Figure 8: Mean hydraulic efficiency of 75 species across 71 sites and five biomes based on the SAPFLUXNET classification. Error bars show the standard error of the mean. Coloured points show different biomes. Colour bands correspond to the five hydraulic efficiency classes shown in Figure 2.

for both beech and Scots pine as a temperate forest and woodland/shrubland were between moderately unrestricted ($\eta = 0.76$ and $\eta = 0.92$, respectively) and unrestricted ($\eta = 1$ and $\eta = 0.8$, respectively), demonstrating a small variability in the efficiency of water transport through SPAC likely due to climate zone and management. Aleppo pine and holm oak, two species widely found in the Mediterranean region, are efficient in managing water resources ($\eta = 0.55$ and $\eta = 0.46$, respectively) confirming adaptation strategies for efficient water regulation, which is important for survival in water-limiting environments.

The implication of this global analysis is twofold. Firstly, it allows comparison between species and provides an index which could be used to identify drought tolerance. Secondly, it allows a quantified evaluation of alternative species choices to underpin decisions for adaptative management under future climate. To date, our understanding of species drought tolerance has focussed

on experiments (Viger et al., 2013; Zhu et al., 2018; Banks and Hirons, 2019), monitoring studies (Feiziasl et al., 2022) or studies using bio-climatic variables (Niinemets and Valladares, 2006; Fuchs et al., 2021b). Standardised databases of water use such as SAPFLUXNET offer the opportunity for exploring a broader range of species. Species with high η are those with levels of transpiration that rarely exceed the available soil water and, from an evolutionary ecological niche perspective, such species have high vulnerability to drought (Choat et al., 2012) and hence will not make the best option for future adaptation.

To improve upon such global analysis, ECT-based hydraulic efficiency needs to be linked more strongly to elements of photosynthesis, carbon uptake and growth. Furthermore, it needs to consider resource competition when trees are in mixtures or alternative uneven-aged canopy structures.

3.5   Further discussion

An important element when considering water movement within plants is stem water storage, which is analogous to capacitance (Zhuang et al., 2014). It is known that capacitance contributes to transpiration during water deficit periods, which can be between 2 and 5% (Salomón et al., 2017). Capacitance, however, is not included in the ECT formulation presented. Electrical circuits analogies of water plant movement are commonly open circuits, with several resistors representing plant parts (e.g., roots, stem, branches and leaves, Landsberg et al., 1976; Milne et al., 1983; Hunt et al., 1991) and with two points of potential difference, soil and leaf. The difference with the ECT formulation is that it represents a closed circuit with the plant depicted as a single resistance. At the same time, the soil is represented not only by a potential but also a resistance. So, the contribution of the stem capacitance is inherently part of the plant resistor.

The ECT based definition of hydraulic efficiency presented in this study is unique in that it considers how efficiently water is transported through the SPAC. Whilst simple concepts of electric theory are presented, it conforms with the theoretical framework set by Sperry and Love (2015) and Sperry et al. (2017) and the conditions identified by Anderegg et al. (2012) regarding the application of water deficit to define when drought-induced mortality occurs. All these approaches follow the fundamental principle of finding the balance point between input and output, supply and loss, or Maximum Power Transfer. So, although supply/loss theory is a good insight into the un-

derline physiological processes, ECT-based hydraulic efficiency offers a practical methodological simplification of broad utility.

ECT-based hydraulic efficiency is easily transferable and applicable for large-scale monitoring of forest drought using modern technology. The reduced cost of robust sensors that collect soil and transpiration data allows long-term deployment across forest stands and regions. Moreover, the continuous monitoring of hydraulic efficiency, combined with other continuous measurements such as dendrometry (Bourbia and Brodribb, 2023) or stable water isotopes (Marshall et al., 2020), offers the opportunity for monitoring water deficit impacts on photosynthesis and growth during naturally occurring droughts or under water exclusion manipulation experiments. Access to global datasets such as those offered by SAPFLUXNET, FLUXNET, and ICOS offer the possibility of assessing the hydraulic efficiency of different ecosystems and species and investigating water deficit impacts on carbon uptake. The application of ECT derived hydraulic efficiency can extend even further into process-based modelling. Integration with either detailed models of water transport or more simplistic yet drought-sensitive models such as the 3PG-SoNWaL model (Morris et al. 2023, in preparation) will provide data for a probabilistic drought risk assessment (van Oijen and Brewer, 2022) based on the SPAC water balance. Finally, ECT-based hydraulic efficiency has the potential for integrating with remote sensing assessments of stand-level (canopy) response as recent developments in improving radar backscatter measurement have the potential to offer a quantification of above-canopy evapotranspiration losses and below-canopy soil moisture.

4   Conclusions

To assess the impact of climate change-induced water deficit on forest function, a reliable monitoring system for its early detection is required. Because assessing the tree or stand resilience is based on understanding the timing, duration, and impact of deficits, it is imperative to develop a simple system that provides reliable and easy application. The Electric Circuit Theory-derived definition of hydraulic efficiency proposed here provides a method for comparing species based on functional water transport and a quantification of drought periodicity. The approach can further advance understanding of the impact of duration and frequency of water deficit events not only on mortality but on the reduction of productivity and the ability to regulate water balance at either the tree or ecosystem level.

Acknowledgements

References

Alizadeh, A., Toudeshki, A., Ehsani, R., Migliaccio, K., Wang, D., 2021. Detecting tree water stress using a trunk relative water content measurement sensor. Smart Agricultural Technology 1, 100003.

URL https://doi.org/10.1016/j.atech.2021.100003

Anderegg, W. R., Berry, J. A., Field, C. B., 12 2012. Linking definitions, mechanisms, and modeling of drought-induced tree death. Trends in Plant Science 17, 693–700.

URL https://linkinghub.elsevier.com/retrieve/pii/S1360138512002130

Arend, M., Link, R. M., Patthey, R., Hoch, G., Schuldt, B., Kahmen, A., 4 2021. Rapid hydraulic collapse as cause of drought-induced mortality in conifers. Proceedings of the National Academy of Sciences of the United States of America 118, e2025251118.

URL https://www.pnas.org/doi/abs/10.1073/pnas.2025251118

Aubinet, M., Hurdebise, Q., Chopin, H., Debacq, A., Ligne, A. D., Heinesch, B., Manise, T., Vincke, C., 2018. Inter-annual variability of Net Ecosystem Productivity for a temperate mixed forest: A predominance of carry-over effects? Agricultural and Forest Meteorology 262, 340–353.

URL https://doi.org/10.1016/j.agrformet.2018.07.024

Banks, J. M., Hirons, A. D., 2019. Alternative methods of estimating the water potential at turgor loss point in acer genotypes. Plant Methods 15, 10–15.

URL https://doi.org/10.1186/s13007-019-0410-3

Bateman, I. J., Anderson, K., Argles, A., Belcher, C., Betts, R. A., Binner, A., Brazier, R. E., Cho, F. H. T., Collins, R. M., Day, B. H., Duran-Rojas, C., Eisenbarth, S., Gannon, K., Gatis, N., Groom, B., Hails, R., Harper, A. B., Harwood, A., Hastings, A., Heard, M. S., Hill, T. C., Inman, A., Lee,

C. F., Luscombe, D. J., MacKenzie, A. R., Mancini, M. C., Morison, J. I. L., Morris, A., Quine, C. P., Snowdon, P., Tyler, C. R., Vanguelova, E. I., Wilkinson, M., Williamson, D., Xenakis, G., 5 2022. A review of planting principles to identify the right place for the right tree for 'net zero plus' woodlands: Applying a place-based natural capital framework for sustainable, efficient and equitable (SEE) decisions. People and Nature.

URL https://onlinelibrary.wiley.com/doi/10.1002/pan3.10331

Beadle, C. L., Turner, N. C., Jarvis, P. G., 1978. Critical water potential for stomatal closure in Sitka spruce. Physiologia Plantarum 43, 160–165.

Beauchamp, K., Mencuccini, M., Perks, M., Gardiner, B., 2013. The regulation of sapwood area, water transport and heartwood formation in Sitka spruce. Plant Ecology and Diversity 6, 45–56.

Bourbia, I., Brodribb, T. J., 3 2023. A new technique for monitoring plant transpiration under field conditions using leaf optical dendrometry. Agricultural and Forest Meteorology 331, 109328.

URL https://linkinghub.elsevier.com/retrieve/pii/S0168192323000229

Brodribb, T. J., Cochard, H., 2009. Hydraulic failure defines the recovery and point of death in water-stressed conifers. Plant Physiology 149, 575–584.

Burgess, S., Downey, A., 5 2014. SFM1 Sap Flow Meter Manual.

Burgess, S. S., Adams, M. A., Turner, N. C., Beverly, C. R., Ong, C. K., Khan, A. A., Bleby, T. M., 2001. An improved heat pulse method to measure low and reverse rates of sap flow in woody plants. Tree Physiology 21, 589–598.

Carminati, A., Javaux, M., 2020. Soil Rather Than Xylem Vulnerability Controls Stomatal Response to Drought. Trends in Plant Science 25, 868–880.

URL https://doi.org/10.1016/j.tplants.2020.04.003

Choat, B., Brodribb, T. J., Brodersen, C. R., Duursma, R. A., López, R., Medlyn, B. E., 2018. Triggers of tree mortality under drought. Nature 558, 531–539.

Choat, B., Jansen, S., Brodribb, T. J., Cochard, H., Delzon, S., Bhaskar, R., Bucci, S. J., Feild, T. S., Gleason, S. M., Hacke, U. G., Jacobsen, A. L., Lens, F., Maherali, H., Martínez-Vilalta, J., Mayr, S., Mencuccini, M., Mitchell, P. J., Nardini, A., Pittermann, J., Pratt, R. B., Sperry, J. S.,

Westoby, M., Wright, I. J., Zanne, A. E., 11 2012. Global convergence in the vulnerability of forests to drought. Nature 491, 752–755.

URL http://www.nature.com/articles/nature11688

Ciruzzi, D. M., Loheide, S. P., 11 2019. Monitoring tree sway as an indicator of water stress. Geophysical Research Letters 46, 12021–12029.

Dickson, B. G., Albano, C. M., Anantharaman, R., Beier, P., Fargione, J., Graves, T. A., Gray, M. E., Hall, K. R., Lawler, J. J., Leonard, P. B., Littlefield, C. E., Mcclure, M. L., Novembre, J., Schloss, C. A., Schumaker, N. H., Shah, V. B., Theobald, D. M., 2018. Circuit-theory applications to connectivity science and conservation. Conservation Biology 0, 1–11.

URL www.circuitscape.org

Drechsler, K., Kisekka, I., Upadhyaya, S., 5 2019. A comprehensive stress indicator for evaluating plant water status in almond trees. Agricultural Water Management 216, 214–223.

Feiziasl, V., Jafarzadeh, J., Sadeghzadeh, B., Shalmani, M. A. M., 3 2022. Water deficit index to evaluate water stress status and drought tolerance of rainfed barley genotypes in cold semi-arid area of Iran. Agricultural Water Management 262.

Fuchs, S., Leuschner, C., Link, R. M., Schuldt, B., 2021a. Hydraulic variability of three temperate broadleaf tree species along a water availability gradient in central Europe. New Phytologist 231, 1387–1400.

Fuchs, S., Schuldt, B., Leuschner, C., 2021b. Identification of drought-tolerant tree species through climate sensitivity analysis of radial growth in central european mixed broadleaf forests. Forest Ecology and Management 494, 119287.

URL https://doi.org/10.1016/j.foreco.2021.119287

Granier, A., Loustau, D., Bréda, N., 12 2000. A generic model of forest canopy conductance dependent on climate, soil water availability and leaf area index. Annals of Forest Science 57, 755–765.

URL http://www.edpsciences.org/10.1051/forest:2000158

Grossiord, C., Buckley, T. N., Cernusak, L. A., Novick, K. A., Poulter, B., Siegwolf, R. T. W., Sperry, J. S., McDowell, N. G., 6 2020. Plant responses to rising vapor pressure deficit. New Phytologist

226, 1550–1566.

URL https://onlinelibrary.wiley.com/doi/10.1111/nph.16485

Hunt, E. R., Running, S. W., Federer, C. A., 1991. Extrapolating plant water flow resistances and capacitances to regional scales. Agricultural and Forest Meteorology 54, 169–195.

Irvine, J., Perks, M. P., Magnani, F., Grace, J., 1998. The response of pinus sylvestris to drought: Stomatal control of transpiration and hydraulic conductance. Tree Physiology 18, 393–402.

Jones, H. G., 1992. Plants and microclimate: A quantitative approach to environmental plant physiology. Cambridge University Press.

Konings, A. G., Saatchi, S. S., Frankenberg, C., Keller, M., Leshyk, V., Anderegg, W. R., Humphrey, V., Matheny, A. M., Trugman, A., Sack, L., Agee, E., Barnes, M. L., Binks, O., Cawse-Nicholson, K., Christoffersen, B. O., Entekhabi, D., Gentine, P., Holtzman, N. M., Katul, G. G., Liu, Y., Longo, M., Martinez-Vilalta, J., McDowell, N., Meir, P., Mencuccini, M., Mrad, A., Novick, K. A., Oliveira, R. S., Siqueira, P., Steele-Dunne, S. C., Thompson, D. R., Wang, Y., Wehr, R., Wood, J. D., Xu, X., Zuidema, P. A., 12 2021. Detecting forest response to droughts with global observations of vegetation water content. Global Change Biology 27, 6005–6024.

Kramp, R. E., Liancourt, P., Herberich, M. M., Saul, L., Weides, S., Tielbörger, K., Májeková, M., 9 2022. Functional traits and their plasticity shift from tolerant to avoidant under extreme drought. Ecology.

URL https://onlinelibrary.wiley.com/doi/10.1002/ecy.3826

Landsberg, J. J., Blanchard, T. W., Warrit, B., 1976. Studies on the movement of water through apple trees. Journal of Experimental Botany 27, 579–596.

Losso, A., Challis, A., Gauthey, A., Nolan, R. H., Hislop, S., Roff, A., Boer, M. M., Jiang, M., Medlyn, B. E., Choat, B., 12 2022. Canopy dieback and recovery in Australian native forests following extreme drought. Scientific Reports 12, 21608.

URL https://www.nature.com/articles/s41598-022-24833-y

Marshall, J. D., Cuntz, M., Beyer, M., Dubbert, M., Kuehnhammer, K., 4 2020. Borehole Equilibration: Testing a New Method to Monitor the Isotopic Composition of Tree Xylem Water in situ. Frontiers in Plant Science 11.

Martínez-Vilalta, J., Poyatos, R., Aguadé, D., Retana, J., Mencuccini, M., 2014. A new look at water transport regulation in plants. New Phytologist 204, 105–115.

McDowell, N., Pockman, W. T., Allen, C. D., Breshears, D. D., Cobb, N., Kolb, T., Plaut, J., Sperry, J., West, A., Williams, D. G., Yepez, E. A., 2008. Mechanisms of plant survival and mortality during drought: Why do some plants survive while others succumb to drought? New Phytologist 178, 719–739.

McRae, B. H., Beier, P., 2007. Circuit theory predicts gene flow in plant and animal populations. PNAS December 11.
URL www.pnas.orgcgidoi10.1073pnas.0706568104

McRae, B. H., Dickson, B. G., Keitt, T. H., Shah, V. B., 2008. Using circuit theory to model connectivity in ecology, evolution, and conservation. Concepts & synthesis emphasizing new ideas to stimulate research in ecology 89, 2712–2724.

Mencuccini, M., Manzoni, S., Christoffersen, B., 5 2019. Modelling water fluxes in plants: from tissues to biosphere. New Phytologist 222, 1207–1222.
URL https://onlinelibrary.wiley.com/doi/10.1111/nph.15681

Milne, R., Ford, E., Deans, J., 1983. Time lags in the water relations of sitka spruce. Forest Ecology and Management 5, 1–25.

Morris, A., Xenakis, G., Perks, M., 2023. Developing the drought-sensitive model 3PG-SoNWaL: evaluating its sensitivity during the 2018 drought for a Sitka spruce stand. In prepration.

Nadezhdina, N., 1999. Sap flow index as an indicator of plant water status. Tree Physiology 19, 885–891.

Nel, A. A., Berliner, P. R., 1 1990. Quantifying leaf water potential for scheduling irrigation of wheat under specific soil-climate conditions. South African Journal of Plant and Soil 7, 68–71.

Nieto, H., Alsina, M., Kustas, W., García-Tejera, O., Chen, F., Bambach, N., Gao, F., Alfieri, J., Hipps, L., Prueger, J., Castro, S., Dokoozlian, N., 2022. Evaluating different metrics from the thermal-based two-source energy balance model for monitoring grapevine water stress. Irrigation Science.

Niinemets, U., Valladares, F., 11 2006. Tolerance to shade, drought, and waterlogging of temperate Northern Hemisphere trees and shrubs. Ecological Monographs 76, 521–547.

Poyatos, R., Granda, V., Flo, V., Adams, M. A., Adorján, B., Aguadé, D., Aidar, M. P. M., Allen, S., Alvarado-Barrientos, M. S., Anderson-Teixeira, K. J., Aparecido, L. M., Arain, M. A., Aranda, I., Asbjornsen, H., Baxter, R., Beamesderfer, E., Berry, Z. C., Berveiller, D., Blakely, B., Boggs, J., Bohrer, G., Bolstad, P. V., Bonal, D., Bracho, R., Brito, P., Brodeur, J., Casanoves, F., Chave, J., Chen, H., Cisneros, C., Clark, K., Cremonese, E., Dang, H., David, J. S., David, T. S., Delpierre, N., Desai, A. R., Do, F. C., Dohnal, M., Domec, J.-C., Dzikiti, S., Edgar, C., Eichstaedt, R., El-Madany, T. S., Elbers, J., Eller, C. B., Euskirchen, E. S., Ewers, B., Fonti, P., Forner, A., Forrester, D. I., Freitas, H. C., Galvagno, M., Garcia-Tejera, O., Ghimire, C. P., Gimeno, T. E., Grace, J., Granier, A., Griebel, A., Guangyu, Y., Gush, M. B., Hanson, P. J., Hasselquist, N. J., Heinrich, I., Hernandez-Santana, V., Herrmann, V., Höltta, T., Holwerda, F., Irvine, J., Isarangkool Na Ayutthaya, S., Jarvis, P. G., Jochheim, H., Joly, C. A., Kaplick, J., Kim, H. S., Klemedtsson, L., Kropp, H., Lagergren, F., Lane, P., Lang, P., Lapenas, A., Lechuga, V., Lee, M., Leuschner, C., Limousin, J.-M., Linares, J. C., Linderson, M.-L., Lindroth, A., Llorens, P., López-Bernal, A., Loranty, M. M., Lüttschwager, D., Macinnis-Ng, C., Maréchaux, I., Martin, T. A., Matheny, A., McDowell, N., McMahon, S., Meir, P., Mészáros, I., Migliavacca, M., Mitchell, P., Mölder, M., Montagnani, L., Moore, G. W., Nakada, R., Niu, F., Nolan, R. H., Norby, R., Novick, K., Oberhuber, W., Obojes, N., Oishi, A. C., Oliveira, R. S., Oren, R., Ourcival, J.-M., Paljakka, T., Perez-Priego, O., Peri, P. L., Peters, R. L., Pfautsch, S., Pockman, W. T., Preisler, Y., Rascher, K., Robinson, G., Rocha, H., Rocheteau, A., Röll, A., Rosado, B. H. P., Rowland, L., Rubtsov, A. V., Sabaté, S., Salmon, Y., Salomón, R. L., Sánchez-Costa, E., Schäfer, K. V. R., Schuldt, B., Shashkin, A., Stahl, C., Stojanović, M., Suárez, J. C., Sun, G., Szatniewska, J., Tatarinov, F., Tesař, M., Thomas, F. M., Tor-ngern, P., Urban, J., Valladares, F., van der Tol, C., van Meerveld, I., Varlagin, A., Voigt, H., Warren, J., Werner, C., Werner, W., Wieser, G., Wingate, L., Wullschleger, S., Yi, K., Zweifel, R., Steppe, K., Mencuccini, M., Martínez-Vilalta, J., 2021. Global transpiration data from sap flow measurements: the SAPFLUXNET database. Earth System Science Data 13 (6), 2607–2649.

URL https://essd.copernicus.org/articles/13/2607/2021/

Rehschuh, R., Cecilia, A., Zuber, M., Faragó, T., Baumbach, T., Hartmann, H., Jansen, S., Mayr,

S., Ruehr, N., 2020. Drought-induced xylem embolism limits the recovery of leaf gas exchange in Scots pine. Plant Physiology 184, 852–864.

Reinert, S., Bögelein, R., Thomas, F., 2012. Use of thermal imaging to determine leaf conductance along a canopy gradient in European beech (Fagus sylvatica). Tree Physiology 32, 294–302.

Rowland, L., Costa, A. C. D., Galbraith, D. R., Oliveira, R. S., Binks, O. J., Oliveira, A. A., Pullen, A. M., Doughty, C. E., Metcalfe, D. B., Vasconcelos, S. S., Ferreira, L. V., Malhi, Y., Grace, J., Mencuccini, M., Meir, P., 2015. Death from drought in tropical forests is triggered by hydraulics not carbon starvation. Nature 528, 119–122.

Salomón, R. L., Limousin, J. M., Ourcival, J. M., Rodríguez-Calcerrada, J., Steppe, K., 2017. Stem hydraulic capacitance decreases with drought stress: implications for modelling tree hydraulics in the Mediterranean oak Quercus ilex. Plant Cell and Environment 40, 1379–1391.

Saxton, K. E., Rawls, W. J., Romberger, J. S., Papendick, R. I., 1986. Estimating soil water characteristics-hydraulic conductivity. Soil Science Society of America Journal 5, 1031–1036.

Schumann, K., Leuschner, C., Schuldt, B., 10 2019. Xylem hydraulic safety and efficiency in relation to leaf and wood traits in three temperate Acer species differing in habitat preferences. Trees - Structure and Function 33, 1475–1490.

Sperry, J. S., Love, D. M., 7 2015. What plant hydraulics can tell us about responses to climate-change droughts. New Phytologist 207, 14–27.
URL https://onlinelibrary.wiley.com/doi/10.1111/nph.13354

Sperry, J. S., Venturas, M. D., Anderegg, W. R., Mencuccini, M., Mackay, D. S., Wang, Y., Love, D. M., 2017. Predicting stomatal responses to the environment from the optimization of photosynthetic gain and hydraulic cost. Plant Cell and Environment 40, 816–830.

Tang, J., Riley, W. J., Marschmann, G. L., Brodie, E. L., 10 2021. Conceptualizing biogeochemical reactions with an Ohm's law analogy. Journal of Advances in Modeling Earth Systems 13.

USDA, 1987. Soil mechanics level 1, module 3. USDA textural classification study guide.

van Oijen, M., Brewer, M., 2022. Probabilistic Risk Analysis and Bayesian Decision Theory.

Springer International Publishing.

URL https://link.springer.com/10.1007/978-3-031-16333-3

Viger, M., Rodriguez-Acosta, M., Rae, A. M., Morison, J. I., Taylor, G., 12 2013. Toward improved drought tolerance in bioenergy crops: Qtl for carbon isotope composition and stomatal conductance in populus. Food and Energy Security 2, 220–236.

Williams, M., Law, B. E., Anthoni, P. M., Unsworth, M. H., 2001. Use of a simulation model and ecosystem flux data to examine carbon-water interactions in ponderosa pine. Tree Physiology 21, 287–298.

Xenakis, G., Ash, A., Siebicke, L., Perks, M., Morison, J. I., 2021. Comparison of the carbon, water, and energy balances of mature stand and clear-fell stages in a British Sitka spruce forest and the impact of the 2018 drought. Agricultural and Forest Meteorology 306 (November 2020), 108437.

URL https://doi.org/10.1016/j.agrformet.2021.108437

Yang, J., Magney, T., Yan, D., Knowles, J., Smith, W., Scott, R., Barron-Gafford, G., 2020. The Photochemical Reflectance Index (PRI) captures the ecohydrologic sensitivity of a semiarid mixed conifer forest. Journal of Geophysical Research: Biogeosciences 125.

Zhou, S., Zhang, Y., Williams, A. P., Gentine, P., 1 2019. Projected increases in intensity, frequency, and terrestrial carbon costs of compound drought and aridity events. Science Advances 5.

URL https://www.science.org/doi/10.1126/sciadv.aau5740

Zhu, S. D., Chen, Y. J., Ye, Q., He, P. C., Liu, H., Li, R. H., Fu, P. L., Jiang, G. F., Cao, K. F., 5 2018. Leaf turgor loss point is correlated with drought tolerance and leaf carbon economics traits. Tree Physiology 38, 658–663.

Zhuang, J., Yu, G. R., Nakayama, K., 2014. A series RCL circuit theory for analyzing non-steady-state water uptake of maize plants. Scientific Reports 4.

Zweifel, R., Zimmermann, L., Newbery, D. M., 2005. Modeling tree water deficit from microclimate: An approach to quantifying drought stress. Tree Physiology 25, 147–156.